



Fermi-LAT analysis and upper-limit calculations for AE Aquarii

H.J. van Heerden and P.J. Meintjes

Department of Physics, University of the Free State, Bloemfontein, South Africa
e-mail: vanheerdenhj@ufs.ac.za

Abstract. The search for gamma-ray emission from AE Aquarii using Fermi-LAT data will be considered. The motivation for the analysis was due to a gap in the SED for AE Aquarii between hard X-rays and reported VHE (TeV) gamma-ray emission from AE Aquarii. The Fermi-LAT analysis and results will be discussed as well as subsequent upper-limit calculations. An updated SED will be shown and a conclusion on the relevance and future studies.

Key words. instrumentation: Fermi-LAT, data-analysis software: Fermi-Sciencetools, stars: Cataclysmic variables, AE Aquarii

1. Introduction

1.1. General model

AE Aquarii is a peculiar nova-like variable star, consisting of a fast rotating white dwarf (WD) primary star, with a rotation period of $P_{\text{spin}} \approx 33$ s orbiting a KIV-type secondary star about the common centre of mass with an orbital period of $P_{\text{orb}} = 9.88$ h. The inferred distance to AE Aquarii is approximately $D \sim 100$ pc (e.g. Welsh et al. 1995; Friedjung 1997).

AE Aquarii evolved into the cataclysmic variable phase after a history of high thermal time-scale mass transfer from the KIV secondary star, and resultant high mass accretion on to the surface of an initially slow rotating white dwarf. The initial rotation period of the magnetized white dwarf during the phase of high mass accretion was $P_{1,i} \sim 1$ h (Meintjes 2002). The current short $P_1 = P_{\text{spin}} \approx 33$ s spin period of the white dwarf and the long $P_{\text{orb}} = 9.88$ h orbital period can be associated with a history of very high, runaway mass ac-

cretion onto the white dwarf, which probably lasted for a period of approximately $t_{\text{acc}} \approx 10^4 - 10^5$ years (Meintjes 2002). In this high mass transfer phase, AE Aquarii could have been a supersoft X-ray source. The high mass accretion rate onto the surface of the white dwarf resulted in the white dwarf being spun-up to a period close to $P_1 = P_{\text{spin}}$ (Meintjes & Venter 2005).

The lack of correlation between the amplitude of the 33 s spin and the increased brightening during flares, and the lack of double peak emission lines, indicates that no accretion disc facilitates mass accretion onto the white dwarf in quiescence and flares. Circular polarization at the level of $(0.05 \pm 0.01) \%$ and $(0.06 \pm 0.01) \%$ was reported by Cropper (1986) and Beskrovnaya et al. (1996) respectively in optical frequencies, which if produced by cyclotron emission, may indicate a magnetic field in excess of $B_1 \sim 10^6$ G (Meintjes & Venter 2005). The fast rotating magnetosphere of the white dwarf acts as a propeller, ejecting

the mass flow from the system before it can settle in a well-defined disc (Wynn et al. 1997).

This propeller effect contributes to the uniqueness of AE Aquarii among the magnetic cataclysmic variables. Another aspect contributing to the uniqueness of AE Aquarii is the highly variable optical as well as non-thermal radiation (Meintjes & Venter 2005). This model integrates the propeller ejection of material by the fast rotating WD with the highly transient thermal and non-thermal emission.

This model then also shows that the violent interaction between the fast rotating magnetosphere and a clumpy fragmented stream results in the growth of unstable modes in the Kelvin-Helmholtz instability and associated turbulence, over length scales comparable to the stream radius. The turbulence in the flow cascades down to the dissipative level over time scales $\tau \sim 3$ hours. If then released through dissipative shocks, this reservoir can drive a luminosity of $L \sim 10^{33}$ erg.s⁻¹, which can significantly contribute to the total emission when blobs collide in the exit stream, resulting in shock heating and associated flares. The propeller can then also accelerate particles, which can explain the other emissions observed. The convergence of these ejected magnetized clouds may result in a radio remnant, like a supernova remnant, surrounding AE Aquarii, which is optically thin in the ultra high frequency range (Meintjes & Venter 2005).

1.2. X-ray and gamma-ray emission

The first scientifically significant work done on AE Aquarii in the high energy (HE) region was the discovery of the 33 second coherent oscillations as presented by Patterson et al. (1980) using *Einstein* data. Subsequent observations and detections were made using *ASCA*, *XMM-Newton*, *Chandra*, *Swift* and *Suzaku*. The x-ray component is both Hard and Soft. The soft x-ray (≤ 10 keV) component is thermal whereas the hard x-ray (≥ 10 keV) component is perhaps non-thermal, (e.g. Choi et al. 1999). More recent studies using the mentioned data-sets was by Oruru & Meintjes (2012) (*Swift* and

Suzaku) who modeled the hard and soft components and how it fits within the SED of AE Aquarii, and Mauche (2006) (*ASCA*, *XMM-Newton* and *Chandra*) who calculated the spin ephemeris of the WD and found a \dot{P} component concluding that the system is braking harder.

Gamma-ray work on AE Aquarii includes announcements by Meintjes et al. (1992, 1994) and Chadwick et al. (1995) of optical like VHE gamma-ray pulsed emission. Search for TeV emission using the *Whipple* 10 m telescope was done by Lang et al. (1998), but no evidence was found for any steady, pulsed or episodic emission. Follow-up work was done by Sidro et al. (2008) using the *MAGIC* telescope, but again no evidence of any steady TeV gamma-ray emission was found. A multi-wavelength campaign was also conducted by López-Coto et al. (2013); Aleksić et al. (2014) in 2012 using data from optical, UV, X-ray (*Swift*) and gamma-ray (*MAGIC*) telescopes. A search for steady TeV as well as variable TeV emission during high states and specifically pulsed emission at 33.08 and 16.54 seconds, did not result in any significant detections. The campaign however did result in upper-limit values for AE Aqr of 6.39×10^{-12} cm⁻²s⁻¹ above 250 GeV and 7.401×10^{-13} cm⁻²s⁻¹ above 1 TeV for a power-law spectrum of -2.6.

All of the above-mentioned gamma-ray work was done using Cerenkov radiation detection systems. With the relatively young space based gamma-ray telescopes like *Fermi* and *AGILE*, the amount of data available to analyse for possible detection of steady, pulsed or episodic emission increases. Fermi-LAT data were therefore considered for analysis in the search for gamma-ray emission from AE Aquarii.

The Fermi Gamma-ray Space Telescope was launched by NASA on 11 June 2008 into a low earth orbit (LEO) at 550 km. The primary instrument on Fermi is the Large Area Telescope (LAT), with a field of view (FOV) that covers about 20% of the sky. Fermi is predominantly in survey mode and covers the whole gamma-ray sky every 3 hours. The LAT has a very large energy sensitivity range, from

20 MeV – 300 GeV. Refer to Atwood et al. (2009) for more detailed discussions on the Fermi-LAT and extended technical specifications. More general information, data archive access and software tools as well as help and support in the form of tutorials and the Fermi “Cicerone” can be accessed through Fermi at ASDC (<http://fermi.asdc.asi.it/>) and Fermi Science Support Center at HEASARC (from here on Fermi.HEASERC, <http://fermi.gsfc.nasa.gov/ssc/>).

2. Fermi-LAT likelihood analysis

The following procedure was applied during the search for possible detection of gamma-ray emission from AE Aquarii using Fermi data. First a search through Fermi-LAT data was done by scanning the Fermi-LAT catalogs for any possible source detections in and around the region centered on AE Aquarii. Fermi has a few notable source detections within the region as listed in Table 1.

The Fermi data-archive was therefore the next point of interest. A “LAT Data Query” on the Fermi.HEASERC site was completed. The search criteria for extraction from the Fermi-LAT database was set to a region centered around AE Aquarii (310.04, -0.87, J2000). A whole range of different datasets were extracted using region of interest (ROI) sizes of 15 and 30 degrees, and the energy ranges set between 100 - 300 000 MeV and in subsets for analysis of different energy bins. The time frame of the data query was set to the maximum time available at the time of extraction, namely 239557417 - END (MET) or 2008-08-04 - END. With MET standing for Mission Elapsed Time.

The analysis and search for gamma-ray emission from AE Aquarii was started by first doing a binned likelihood analysis. The events files were filtered as follows: The energy range under consideration was set between 100-300 000 MeV for $evclass = 2$. The value for the $evclass$ is based on the fact that for LAT Pass 7 data the source events are specified as event class 2. The ROI Radius was set to 15 degrees at a zenith angle of 100 degrees

with a pixel scale defined as 0.1 degrees/pixel resulting in a resolution of 150×150 pixels.

The latest background models available at the time was used along with a source model file created using the available tools and resources. See Fig. 1 for the completed binned likelihood analysis model map image for the total time.

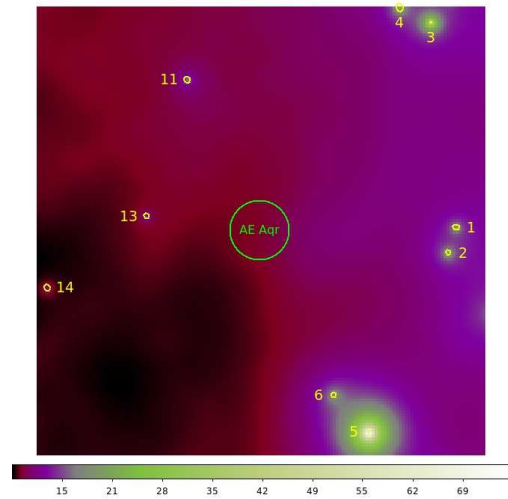


Fig. 1. Test likelihood analysis map centered about AE Aquarii

The region encircled in green is centered on AE Aquarii, while the known sources from the 2nd Fermi Catalog are encircled in yellow and numbered according to Table 1. The size of the circles are inversely proportional to the probability of the likelihood analysis model, i.e. the smaller the circle the better the model fitted for the detected source, or the stronger the source’s gamma-ray emission. As can be seen no statistical significant source (actually no source whatsoever) has been detected at the target coordinates for AE Aquarii. For this reason the size of the circle was set to 2 degrees (which is the size of the error box for Fermi-LAT sources as listed in the Fermi-LAT source catalog). Based on the visual results obtained, no conclusive argument could be made for a positive detection of any steady continuous gamma-ray emission from AE Aquarii.

Table 1. List of objects from the 2nd Fermi Catalog.

Number	Source Name	RA (J2000)	Dec (J2000)	Optical
1	2FGLJ2014.0-0046	20 14 04.0	-00 46 17.1	BL Lac
2	2FGLJ2015.1-0137	20 15 06.7	-01 37 11.1	BL Lac
3	2FGLJ2017.3+0603	20 17 23.8	+06 03 14.1	Pulser
4	2FGLJ2021.5+0632	20 21 33.7	+06 32 31.0	Unassociated
5	2FGLJ2025.6-0736	20 25 39.7	-07 36 18.6	FSRQ
6	2FGLJ2030.3-0622	20 30 22.3	-06 22 21.6	FSRQ
11	2FGLJ2050.0+0408	20 50 00.7	+04 08 59.3	BL Lac
13	2FGLJ2055.4-0023	20 55 26.5	-00 23 52.8	BL Lac
14	2FGLJ2108.7-0246	21 08 43.1	-02 46 48.2	BL Lac

Therefore additional source detection methods were used.

3. Periodogram analysis

With the results from the likelihood analysis indicating no statistically significant detection, the assumption can be made that if there is any gamma-ray emission from AE Aquarii, it will be at the noise level. Therefore an analysis of the noise profile and structures has to be considered.

Because of the known first and second harmonic periodicity of 33.08 (30.23 mHz) and 16.54 (60.459 mHz) seconds for the rapidly spinning WD (that is detectable from Optical to X-ray), the argument can be made that a periodicity search in the gamma-ray data centered around AE Aquarii can be used to possibly identify a statistically significant detection, and therefore possible identification of a Gamma-ray signal and a search for a production mechanism. This was done with the following technique. As mentioned in the previous section, a series of Fermi energy bins were downloaded from the Fermi_HEASERC site as well as the latest Space-craft file. The bins were 100-250 MeV, 250-500 MeV, 500-750 MeV, 750-1000 MeV, 1-10 GeV, 1-100 GeV and 1-300 GeV. The bins were chosen to make modular analysis possible, i.e. to try and exclude galactic background noise contamination at lower energies, and lack of count levels at high energies. Each energy bin was then used to construct periodograms using the

“gtpsearch” tool available in the Fermi science tools package. A Rayleigh analysis was done with the step size at 5000 times the Fourier resolution (considering the very long time baseline of the datasets), and the number of trials set at 2000, centered on about 40 mHz to cover the frequencies from 10-70 mHz centered on the coordinates for AE Aquarii.

The resultant periodograms were then analysed for signal/noise significance. Using the assumption that Periodogram power peak distribution levels below 4σ can be considered as noise, the power peaks greater than 4σ were sampled and analysed for signal/noise significance. This analysis method was applied to each power bin. The newly sampled power peaks greater than 4σ from the periodograms of the separate energy bins were then combined. This was done with the assumption that possible signal peaks will have components in a greater number of the bins, while noise patterns will have a more random distribution. This will lead to a boost in signal peak power, and a drop in noise peak power. The final resultant Periodogram can then be considered for signal detection tests (See Fig. 2).

As can be seen from the figure, there appears to be a power peak at the current ephemeris model position for the second harmonic at 60.46 mHz as indicated with the red line. The question of if this peak is a possible signal peak can only be considered through further analysis of the nature of the stronger peaks surrounding it. By plotting a

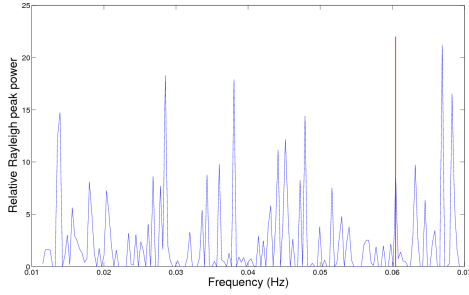


Fig. 2. Combined Periodogram of the relative Rayleigh peak power above 4σ . The current model ephemeris for AE Aquarii is shown in red.

histogram of the peak distribution in terms of the Rayleigh power z , a noise profile versus peak power can be made. A combined histogram for all datasets considered in the above mentioned analysis was therefore plotted, with the noise profile fitted. (See Fig. 3).

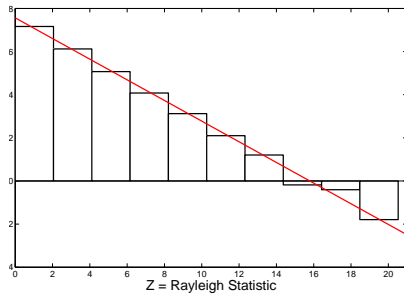


Fig. 3. Combined histogram of the Rayleigh power z for all relevant datasets. Noise profile fit is shown in red.

From the histogram of the Rayleigh power distribution z , a white noise profile trend can be seen at lower powers, with slight deviations at higher power values. Using noise profile studies and power peak distributions (as above) through the different energy bins, as well as comparisons with Periodogram analysis of surrounding areas, signal/noise significance can be analysed. This analysis will be considered in additional studies.

4. Upper-limit calculations and SED

Considering the results obtained from the section above as well as previous studies, an updated spectral energy distribution (SED) can serve as a tool for model parameter investigations. Therefore an updated SED was determined for AE Aquarii that includes the reported optical like VHE pulsed emission as well as the more recent upper-limits as calculated by López-Coto et al. (2013); Aleksie et al. (2014) (Indicated by the blue upper-limit markers). Additionally provisional upper-limits were also calculated for AE Aquarii at energies of 10 GeV and 100 GeV using the LATAnalysisScripts, with values of $3.47 \times 10^{-7} \text{ ph cm}^{-2} \text{ s}^{-1}$ and $3.48 \times 10^{-7} \text{ ph cm}^{-2} \text{ s}^{-1}$ respectively for a delta (loglike) of 1.35 (Indicated by the red upper-limit markers). These were then also included in the SED. The Radio, IR, Optical, UV and X-ray data was obtained from Oruru & Meintjes (2012) and cross-checked with published data from the online Vizier catalogue. Sensitivity curves for selected instruments were also included as obtained from the SED Builder available from ASDC (<http://tools.asdc.asi.it/SED/>). See Fig. 4 for the most recent SED for AE Aquarii.

5. Conclusion

From the preliminary results obtained in this study and in comparison with previously cited studies, it is still inconclusive that any statistically significant detection of gamma-ray emission from AE Aquarii is possible. The calculated upper-limits do give a possible region wherein future studies can be made especially with higher sensitivity instrumentation planned, e.g. CTA. At this stage the possibility of gamma-ray emission from AE Aquarii cannot be ruled out as the highly energetic nature of the system will certainly allow for gamma-ray production mechanisms. The problem faced in terms of current studies is that any emission in the gamma-ray region is at such a low level that it falls within the noise regime of the currently available instruments. Therefore further searches for possible signal

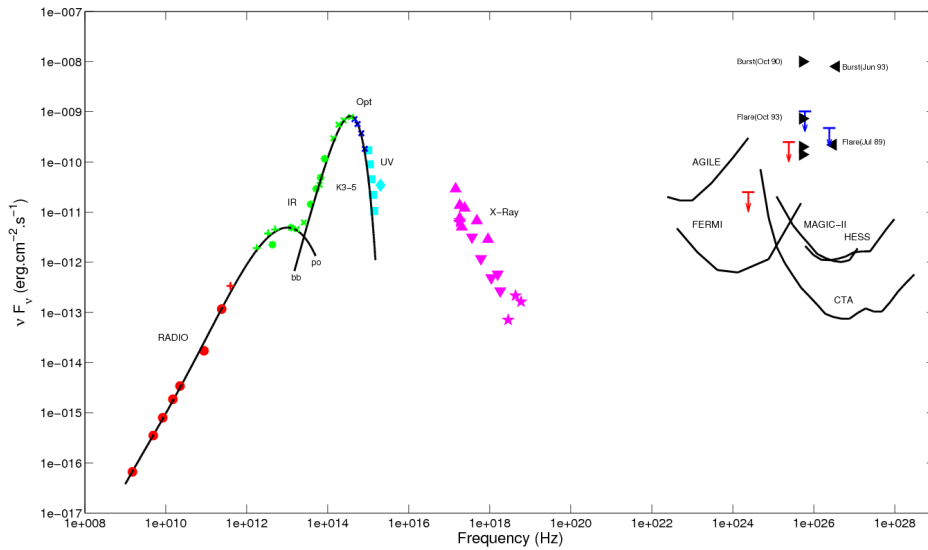


Fig. 4. Spectral energy distribution for AE Aquarii, including the sensitivity curves for selected instruments.

signatures would only be possible through a thorough analysis of the noise distribution and characteristics within the datasets.

Acknowledgements. This research has made use of data, software and/or web tools obtained from NASA's High Energy Astrophysics Science Archive Research Center (HEASARC), a service of Goddard Space Flight Center and the Smithsonian Astrophysical Observatory.

References

- Aleksić, J. et al. 2014, *A&A*, 568, 8
 Atwood, W. B. et al. 2009, *ApJ*, 697, 1071
 Beskrovnaya, N. G. et al. 1996, *A&A*, 307, 840
 Chadwick, P. M., et al. 1995, *Astropart. Phys.*, 4, 99
 Choi, C., et al. 1999, *ApJ*, 525, 399
 Cropper, M. 1986, *MNRAS*, 222, 225
 de Jager, O. C., et al. 1994, *MNRAS*, 267, 577
 Friedjung, M. 1997, *New Astron.*, 2, 319
 Lang, M. J., et al. 1998, *Astropart. Phys.*, 9, 203
 López-Coto, R. et al. 2013, *ArXiv Astrophysics e-prints*, 1309.2503
 Mauche, C. W. 2006, *MNRAS*, 369, 1983
 Meintjes, P. J., et al. 1992, *ApJ*, 401, 325
 Meintjes, P. J., et al. 1994, *ApJ*, 434, 292
 Meintjes, P. J. 2002, *MNRAS*, 336, 265
 Meintjes, P. J. & Venter, L. A. 2005, *MNRAS*, 360, 573
 Oruru, B. & Meintjes, P. J. 2012, *MNRAS*, 421, 1557
 Patterson, J., et al. 1980, *ApJ*, 240, L133
 Sidro, N., et al. 2008, *Proceedings of the 30th International Cosmic Ray Conference*, 2, 715
 Welsh, W.F., et al. 1995, *MNRAS*, 275, 649
 Wynn, G. A., et al. 1997, *MNRAS*, 286, 436